

## Fabrication and Characterization of Topological Insulator $\text{Bi}_2\text{Se}_3$ Nanocrystals

S.Y.F. Zhao<sup>1</sup>, C. Beekman<sup>1</sup>, L.J. Sandilands<sup>1</sup>, J.E.J. Bashucky<sup>1</sup>, D. Kwok<sup>2</sup>, N. Lee<sup>2</sup>, A.D. LaForge<sup>3</sup>, S.W. Cheong<sup>2</sup> and K.S. Burch<sup>1, a)</sup>

<sup>1</sup>*Department of Physics & Institute of Optical Sciences, University of Toronto, 60 St. George Street, Toronto, ON M5S 1A7*

<sup>2</sup>*Rutgers Center for Emergent Materials and Department of Physics and Astronomy, Rutgers University, 136 Frelinghuysen Road, Piscataway, NJ 08854, USA.*

<sup>3</sup>*Department of Physics, University of California, Santa Cruz, 1156 High Street, Santa Cruz, California 95064, USA.*

(Dated: 10 August 2018)

In the recently discovered class of materials known as topological insulators, the presence of strong spin-orbit coupling causes certain topological invariants in the bulk to differ from their values in vacuum. The sudden change of invariants at the interface results in metallic, time reversal invariant surface states whose properties are useful for applications in spintronics and quantum computation. However, a key challenge is to fabricate these materials on the nanoscale appropriate for devices and probing the surface. To this end we have produced 2 nm thick nanocrystals of the topological insulator  $\text{Bi}_2\text{Se}_3$  via mechanical exfoliation. For crystals thinner than 10 nm we observe the emergence of an additional mode in the Raman spectrum. The emergent mode intensity together with the other results presented here provide a recipe for production and thickness characterization of  $\text{Bi}_2\text{Se}_3$  nanocrystals.

Topological metallic surface states are predicted to have numerous properties that are useful for spintronics and quantum computation.<sup>1,2</sup> A challenging aspect of this research has been to isolate surface state contributions to the measured properties of topological insulators<sup>3-7</sup>. Studying nanometer thick crystals allows one to tune the chemical potential with electric field<sup>8-12</sup>, as well as observe modifications of the excitation spectrum produced by interactions of top and bottom surfaces<sup>11,13-16</sup>. One option for producing thin crystals is mechanical exfoliation. This method, together with Raman spectroscopy, has proven to be extremely fruitful in the study of graphene<sup>17,18</sup> and other nanocrystals<sup>19,20</sup>. Indeed, Raman provides direct access to the phonon spectrum and can be used to map the thickness<sup>17,21</sup> or doping level<sup>22</sup> over a large area.

Similar studies of the topological insulators  $\text{Bi}_2\text{Se}_3$  and  $\text{Bi}_2\text{Te}_3$  have been attempted. To date, these experiments have been limited to exfoliated  $\text{Bi}_2\text{Se}_3$  crystals >10 nm thick<sup>12,23,24</sup> or  $\text{Bi}_2\text{Te}_3$  where the bulk gap is small<sup>8,9</sup>. A limiting factor in these experiments was the strong optical absorption of these compounds, making the identification of thin crystals difficult on Si/SiO<sub>2</sub> substrates. With this in mind, we have mechanically exfoliated  $\text{Bi}_2\text{Se}_3$  crystals on Mica, enabling us to optically identify crystals only 2 nm thick. By systematically studying these crystals with Raman spectroscopy and optical and atomic force microscopies (AFM) we have devised a method for characterizing the thickness of  $\text{Bi}_2\text{Se}_3$  nanocrystals using non-invasive, all-optical methods. Specifically, an additional mode appears in the Raman spectra for ultrathin (< 10 nm) crystals. The observed thickness dependence of the emergent mode intensity can be used for thickness verification of nanocrystals via Raman measurements.

$\text{Bi}_2\text{Se}_3$  forms a rhombohedral lattice in which the unit cell is composed of three five-layer stacks known as quintu-

ple layers (QL). A unit cell measures 2.87 nm along the *c* axis, and 1 QL is  $\approx 0.96$  nm thick.<sup>25</sup> Atoms are arranged into planar hexagonal sheets with the sequence  $[\text{Se}^{(2)}\text{-Bi-Se}^{(1)}\text{-Bi-Se}^{(2)}]$ .<sup>26</sup> The superscripts indicate the structural inequivalence of the Se ions, with the  $\text{Se}^{(1)}$  atom at a center of inversion within a QL. Therefore one expects phonon modes to be exclusively infrared (IR) or Raman active. The weak van der Waals bonds between neighboring  $\text{Se}^{(2)}$  planes enables mechanical exfoliation. Ultrathin  $\text{Bi}_2\text{Se}_3$  nanocrystals could be identified after exfoliation by optical microscopy in transmission mode. The crystal thickness was subsequently determined using AFM<sup>26</sup>.

Raman spectroscopy ( $\lambda = 532$  nm, spot size  $\sim 1$   $\mu\text{m}$ ) confirmed that these nanocrystals are indeed  $\text{Bi}_2\text{Se}_3$  and was used to study the evolution of the crystal lattice structure with thickness. A Raman spectrum ( $I(\omega)$ ) for a bulk crystal is shown in Fig. 1a, where we observe a strong phonon mode at  $175\text{ cm}^{-1}$  and the onset of a mode below  $150\text{ cm}^{-1}$ . Previous results<sup>25</sup> suggest the higher energy mode corresponds to a Raman active  $A_{1g}$  mode and the latter to an  $E_g$  mode, in accord with group theory predictions for phonons at the Brillouin zone center ( $q = 0$ ) probed by optical experiments. Indeed, the 5 atoms in the unit cell should lead to 12 optical modes, each of which is either exclusively Raman or infrared active<sup>25</sup>. We also observe a broad shoulder between  $200\text{-}350\text{ cm}^{-1}$ , similar to a feature observed in a recent IR study of bulk  $\text{Bi}_2\text{Se}_3$  (see Fig.2b).<sup>27</sup> The presence of this feature in both Raman as well as IR and its broad lineshape suggest that it is due to two-phonon excitations.

To quantitatively analyze the evolution of the spectra, we fit the measured Raman data with multiple Lorentzian oscillators in the form:  $I(\omega) = I_0 + \sum_i \left( \frac{A_i \Gamma_i}{4(\omega - E_i)^2 + \Gamma_i^2} \right)$  where  $i$  ranges from 1 to 3 or 4, depending on thickness,  $I_0$  accounts for the background,  $E_i$  is the center,  $\Gamma_i$  is the width, and  $A_i$  is the area of peak  $i$ . The resulting fit for the bulk spectrum with three oscillators is shown in Fig. 1a, where the center frequency of the

<sup>a)</sup>Electronic mail: kburch@physics.utoronto.ca

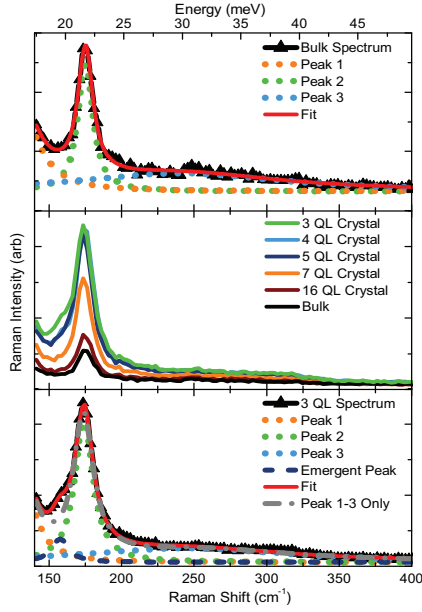


FIG. 1. (Color online) Raman spectra for  $\text{Bi}_2\text{Se}_3$  (a) Spectrum for the bulk crystal (line + symbols) with the corresponding fit (solid line) consisting of three Lorentzian oscillators (dotted lines). (b) Spectra for crystals of varying thicknesses, 3  $\rightarrow$  16 QL and bulk. (c) Spectrum for 3QL nanocrystal. The data (line + symbols) is fit with four Lorentzian oscillators (solid line). The fit resulting from three oscillators is shown for comparison (dashed dotted line).

$E_g$  mode (Peak 1) was fixed at  $131.5 \text{ cm}^{-1}$  based on previous studies<sup>25</sup>. Turning to Fig. 1b we examine the evolution of the Raman spectra with varying crystal thicknesses, where an enhancement of the overall signal is observed with decreasing number of QL. As is discussed below this enhancement results from multiple reflections in the  $\text{Bi}_2\text{Se}_3$  crystal. Perhaps more surprisingly, an additional mode emerges at  $158 \text{ cm}^{-1}$  as the crystal thickness is reduced (see Fig. 1c). Indeed, the use of only three oscillators, which worked well for crystals thicker than 10 QL (Fig. 1a), results in a large difference around  $158 \text{ cm}^{-1}$  between the fit (dashed dotted line) and the spectrum. By simply adding another mode ( $i = 4$ ), the fit (solid line) agrees very well with the data. The emergence of the mode at  $158 \text{ cm}^{-1}$  for ultrathin crystals suggests it can be used to verify sample thickness.

We explore this possibility in Fig. 2, where we plot the ratio of the emergent mode intensity with the main peak intensity ( $\frac{A_4}{A_2}$ ). For thicknesses below 10 QL this ratio increases and agrees well with  $\frac{\alpha}{(QL-2)}$  behavior (dashed line), which corresponds to the relative weight of surface and bulk modes. Indeed, the intensity of a particular mode is proportional to the volume over which the light can emanate. For a surface mode, this volume is independent of thickness. In contrast, for a bulk mode the volume probed is proportional to the crystal thickness (for thicknesses less than the penetration depth). Unfortunately, due to the detection limit of our instrument, we are not able to convincingly detect the mode for  $A_4/A_2 < 0.02$ .

While the mode appears to have its origin in the surface,

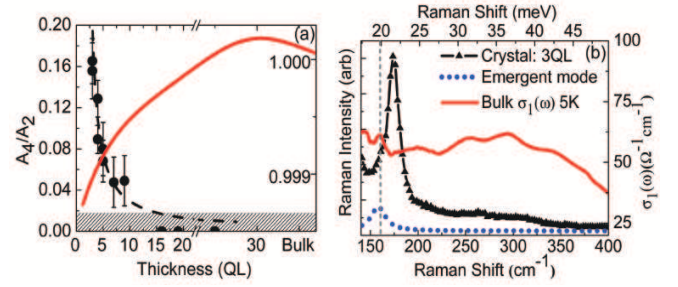


FIG. 2. (Color online) (a) Ratio of emergent peak intensity to the main peak intensity (determined from fits) as function of crystal thickness. The dashed line is a guide to the eye and plotted to show the  $\frac{\alpha}{(QL-2)}$  trend of the ratio. The gray area for  $A_4/A_2 < 0.02$  indicates the detection limit of our system. The ratio  $A_4/A_2$  as function of crystal thickness due to FP effects (solid line, right axis). (b) Left axis: Raman spectrum for a 3QL thick crystal (line + symbols) and the lorentzian corresponding to the emergent mode (dotted line). Right axis: optical conductivity data (solid line) of a bulk  $\text{Bi}_2\text{Se}_3$  single crystal taken at  $T = 5 \text{ K}$ .

it could also be due to Fabry-Perot (FP) interference in the Mica substrate. To rule this out, we repeatedly performed Raman spectroscopy on a single 3 QL nanocrystal and subsequently cleaved the back surface of the Mica to reduce its thickness. The resultant spectra all overlapped (not shown), implying that FP interference in the Mica substrate can be neglected. Nonetheless, for a fixed substrate thickness, the interference effects due to multiple reflections in the  $\text{Bi}_2\text{Se}_3$  nanocrystals will change as the crystals are thinned. To check the FP effects on the Raman spectra we have performed a calculation similar to the one shown to work well in graphene and  $\text{Bi}_2\text{Sr}_2\text{CaCu}_2\text{O}_8$  nanocrystals.<sup>20,21</sup> In Fig. 3, we plot the measured and the calculated intensity (FP model) as a function of crystal thickness for the main mode ( $175 \text{ cm}^{-1}$ ). Changes in the ratio ( $\frac{A_4}{A_2}$ ) due to FP effects are plotted in Fig. 2a and only reveals a very small dependency on crystal thickness, which is opposite to what we observe. Therefore, the emergent mode is intrinsic to  $\text{Bi}_2\text{Se}_3$  nanocrystals and not caused by FP effects. However, Fig.3 shows that the change in the overall Raman signal with crystal thickness is explained by FP interference effects only if the optical constants are modified from the bulk values. This modification is not unreasonable given recent photoemission experiments<sup>14,16</sup>. Interestingly, these data also show the utility of Raman measurements, as the overall intensity can be used to determine the thickness of the  $\text{Bi}_2\text{Se}_3$  nanocrystals.

While the FP interference described above can account for the overall intensity-thickness trends in Fig. 1, the origin of the  $158 \text{ cm}^{-1}$  mode remains unclear. Interestingly, an additional mode also appeared in Raman spectra of nanocrystals of the isostructural topological insulator  $\text{Bi}_2\text{Te}_3$ .<sup>8</sup> This mode matched perfectly the frequency of an infrared-active mode and so it was attributed to the breaking of inversion symmetry. Shahil *et al* suggested that mechanical exfoliation resulted in breaks within a QL as well as between them. A similar explanation may be appropriate for  $\text{Bi}_2\text{Se}_3$ : a recent IR reflectance study of the bulk revealed a mode with the same frequency and width<sup>27</sup> (see Fig.2b). However, in  $\text{Bi}_2\text{Te}_3$  this mode ap-

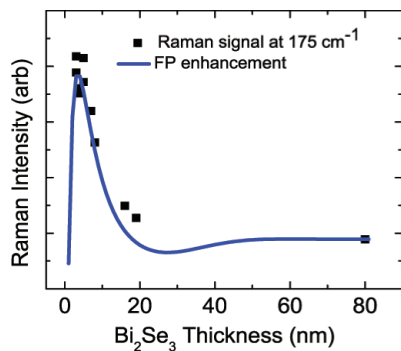


FIG. 3. (Color online) Raman intensities as function of crystal thickness at  $175\text{ cm}^{-1}$  (squares) and calculated Raman intensities due to FP interference effects (solid line: optical constants modified from bulk values).

peared in crystals thinner than 84 nm, whereas it only appears in  $\text{Bi}_2\text{Se}_3$  nanocrystals thinner than 10 nm. We believe the mode may be due to the built-in electric fields at the surface. Specifically, the band bending inherent to materials with surface states will generate an electric field that will break the inversion symmetry.

We have shown that Raman spectroscopy is an effective nanometrology tool for identifying nanocrystals of the topological insulator  $\text{Bi}_2\text{Se}_3$ . This is accomplished by monitoring i) the overall intensity of the Raman signal and/or ii) the strength of the emergent mode at  $158\text{ cm}^{-1}$ . The overall thickness dependence of the intensity can be accounted for by proper modeling of the effect of interference on the Raman spectra. The origin of the emergent mode remains unclear, although the presented optical conductivity data suggests that inversion symmetry breaking leads to an IR mode becoming Raman active. However, it is interesting to note that the emergent mode appears for the same thickness regime of  $\text{Bi}_2\text{Se}_3$  for which a gap has been theorized to open due to coupling of the two surfaces.<sup>14,16</sup> In addition, the polar surface of Mica may lead to band bending, which breaks inversion symmetry. Therefore performing Raman spectroscopy on a suspended crystal would provide conclusive determination of the influence of the Mica substrate on the  $\text{Bi}_2\text{Se}_3$  nanocrystals. Nonetheless, we have provided a path for fabricating and identifying  $\text{Bi}_2\text{Se}_3$  nanocrystals through the combination of mechanical exfoliation on transparent substrates and the use of Raman spectroscopy. This work paves the way for future devices and studies of the surface states of topological insulators.

We are grateful for numerous discussions with Y.B. Kim and H.Y. Kee and we thank Y. J. Choi for the transport measurement. Work at the University of Toronto was supported by NSERC, CFI, and ORF; work at Rutgers University was supported by the NSF under grant NSF-DMR-0804109.

<sup>1</sup>J. Moore *Nat. Phys.*, **5**, 378 (2009)

<sup>2</sup>H. Zhang, C. Liu, X. Qi, X. Dai, Z. Fang, S. Zhang, *Nature Phys.*, **5**, 438–442 (2009) and references therein

<sup>3</sup>H. Peng, K. Lai, D. Kong, S. Meister, Y. Chen, X.-L. Qi, S.-C. Zhang, Z.-X. Shen, Y. Cui, *Nature Mat.*, **9**, 225 (2010)

- <sup>4</sup> K. Eto, Z. Ren, A. A. Taskin, K. Segawa, Y. Ando *Phys. Rev. B*, **81**, 195309 (2010)
- <sup>5</sup> J. G. Analytis, J.-H. Chu, Y. Chen, F. Corredor, R. D. McDonald, Z. X. Shen, I. R. Fisher *Phys. Rev. B*, **81**, 205407 (2010)
- <sup>6</sup> T. Zhang, P. Cheng, X. Chen, J.-F. Jia, X. Ma, K. He, L. Wang, H. Zhang, X. Dai, Z. Fang, X. Xie, Q.-K. Xue, *Phys. Rev. Lett.*, **103**, 266803 (2009)
- <sup>7</sup> S. R. Park, W. S. Jung, C. Kim, D. J. Song, C. Kim, S. Kimura, K. D. Lee, N. Hur, *Phys. Rev. B*, **81**, 041405 (2010)
- <sup>8</sup> K. M. F. Shahil, M. Z. Hossain, D. Teweldebrhan, A. A. Balandin, *Appl. Phys. Lett.*, **96**, 153103 (2010)
- <sup>9</sup> D. Teweldebrhan, V. Goyal, A. A. Balandin *Nano Lett.*, **10**, 1209 (2010)
- <sup>10</sup> Z. Ding, S. K. Bux, D. J. King, F. L. Chang, T.-H. Chen, S.-C. Huang, R. B. Kaner, *Journal of Mat. Chem.*, **19**, 2588 (2009)
- <sup>11</sup> Y. Sakamoto, T. Hirahara, H. Miyazaki, S.-i. Kimura, S. Hasegawa, *Phys. Rev. B*, **81**, 165432 (2010) and references therein
- <sup>12</sup> J. G. Checkelsky, Y. S. Hor, R. J. Cava, N. P. Ong, *arXiv* (2010), arXiv:1003.3883v1 *cond-mat.mes-hall*
- <sup>13</sup> J. Linder, T. Yokoyama, A. Sudbø, *Phys. Rev. B*, **80**, 205401 (2009)
- <sup>14</sup> C.-X. Liu, H. Zhang, B. Yan, X.-L. Qi, T. Frauenheim, X. Dai, Z. Fang, S.-C. Zhang, *Phys. Rev. B*, **81**, 041307 (2010)
- <sup>15</sup> H.-Z. Lu, W.-Y. Shan, W. Yao, Q. Niu, S.-Q. Shen, *Phys. Rev. B*, **81**, 115407 (2010)
- <sup>16</sup> Y. Zhang, K. He, C.-Z. Chang, C.-L. Song, L.-L. Wang, X. Chen, J.-F. Jia, Z. Fang, X. Dai, W.-Y. Shan, S.-Q. Shen, Q. Niu, X.-L. Qi, S.-C. Zhang, X.-C. Ma and Q.-K. Xue, *Nature Phys.*, **6**, 584 (2010)
- <sup>17</sup> A. Gupta, G. Chen, P. Joshi, S. Tadigadapa, P. C. Eklund, *Nano Lett.*, **6**, 2667 (2006)
- <sup>18</sup> A. B. Kuzmenko, L. Benfatto, E. Cappelluti, I. Crassee, D. van der Marel, P. Blake, K. S. Novoselov, A. K. Geim, *Phys. Rev. Lett.*, **103**, 116804 (2009) and references therein
- <sup>19</sup> L. M. Malard, M. A. Pimenta, G. Dresselhaus, M. S. Dresselhaus, *Phys. Rep.*, **473**, 51 (2009)
- <sup>20</sup> L. J. Sandilands, J. X. Shen, G. M. C. F. Zhao, S. Ono, Y. Ando, K. S. Burch, *Phys. Rev. B*, **82**, 064503 (2010)
- <sup>21</sup> D. Yoon, H. Moon, Y.-W. Son, J. S. Choi, B. H. Park, Y. H. Cha, Y. D. Kim, H. Cheong, *Phys. Rev. B*, **80**, 125422 (2009)
- <sup>22</sup> D. M. Basko, S. Piscanec, A. C. Ferrari, *Phys. Rev. B*, **80**, 165413 (2009) and references therein
- <sup>23</sup> H. Steinberg, D. R. Gardner, Y. S. Lee, P. Jarillo-Herrero, *eprint arXiv*, **1003**, 3137 (2010)
- <sup>24</sup> B. Sacepe, J. B. Oostinga, J. Li, A. Ubaldini, N. J. G. Couto, E. Giannini, A. F. Morpurgo, *arXiv:1101.2352v1 [cond-mat.mes-hall]*, (2011)
- <sup>25</sup> W. Richter, C. R. Becker, *Phys. Stat. Sol. (b)*, **84**, 619 (1977)
- <sup>26</sup> See supplementary material at <http://dx.doi.org/10.1063/1.3573868> for the crystal structure of  $\text{Bi}_2\text{Se}_3$  and an AFM image and the thickness

determination.

<sup>27</sup> A. D. Laforge, A. Frenzel, B. C. Pursley, T. Lin, X. Liu, J. Shi, D. N. Basov, *Phys. Rev. B*, **81**, 125120 (2010)